Control of Wind Turbine Based on DFIG Using Fuzzy-PI and Sliding Mode Controllers

B.HAMANE
Department of Electrical and Computer Engineering
Université du Québec à Trois-Rivières, QC, Canada
Bekhada.Hamane@uqtr.ca

M. L. DOUMBIA
Department of Electrical and Computer Engineering
Université du Québec à Trois-Rivières, QC, Canada
Mamadou.Doumbia@uqtr.ca

M. BOUHAMIDA
Department of Electrical Engineering
University Mohamed Boudiaf, Oran, Algeria
m_bouhamida@yahoo.com

M. BENGHANEM
Department of Electrical Engineering
University Mohamed Boudiaf, Oran, Algeria
mbenghanem69@yahoo.fr

***Abstract*—This paper presents the study of a wind energy conversion system (WECS) based on a doubly fed induction generator (DFIG) connected to electric power grid. The performances (reference tracking and robustness) of classical Proportional-Integral (PI), Fuzzy-PI and Sliding Mode (SM) controllers are compared with respect to the wind speed fluctuation and the impact on the produced energy quality. Moreover, direct vector control with stator flux orientation of the DFIG is used to control the active and reactive powers between the stator and the grid. The performances of the system were analyzed and compared by simulation using Matlab/Simulink/SimPower Systems**

Keywords*— *WECS; DFIG; Direct Vector Control; Fuzzy-PI controller; Sliding Mode.

I. INTRODUCTION

Doubly fed induction generator (DFIG) is an electrical three phase asynchronous machine with wound rotor accessible for control. As the power handled by the rotor is proportional to the slip, the power electronic converter used in the rotor circuit can be designed for only a fraction of the overall system power [1]-[2]. This topology is very attractive for both wind energy generation and high power drive applications. Fuzzy logic (FL) based techniques have been proposed for wind power generation control [3].

The FL based controller is capable to embed in the control strategy, the qualitative process's knowledge and experience of an operator or field engineer. However, FL controller has been criticized for its limitations, such as the lack of a formal design methodology, the difficulty in predicting stability and robustness of controlled systems [4]. Then, a controller based on Sliding Mode (SM) method can be used to overcome this drawback. A Sliding Mode controller has been applied in many fields due to its excellent properties, such as insensitivity to some external disturbances and parameters variation, SM controller can exhibit fast dynamic responses [5].

This paper presents a complete comparative analysis of proportional-Integral (PI), Sliding Mode [5] and Fuzzy-PI [6] controllers for doubly-fed induction wind energy conversion system (WECS). Theoretical analysis, modeling and simulation study are provided. Control strategies were developed to control the active and reactive power in order to maximize the wind energy production. The performances of the three control strategies are investigated and compared regarding the reference tracking and the robustness. Figure 1 shows the DFIG wind energy conversion system structure.

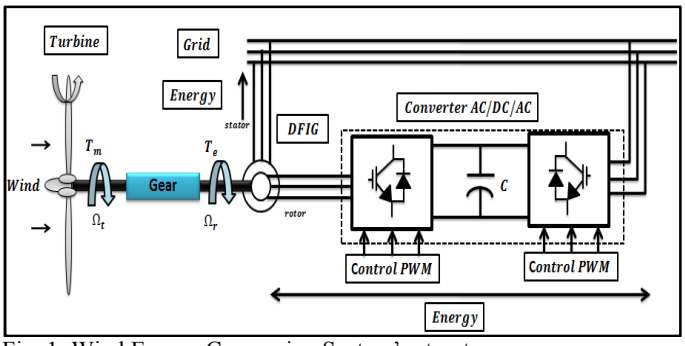

Fig. 1: Wind Energy Conversion System's structure

II. WECS MODELING

A. Wind Turbine Model

The mechanical power transferred from the wind to the aerodynamic rotor is expressed as [8]:

$$P_t = \frac{1}{2}\rho R^2 V^3 C_p(\lambda,\beta) \quad (1)$$

The input torque in the transmission mechanical system is then [8]:

$$T_m = \frac{P_t}{\omega_t} = \frac{\frac{1}{2}C_p(\lambda,\beta)\rho R^2 v^3}{\omega_t} \quad (2)$$

978-1-4799-3787-5/14/$31.00 ©2014 IEEE

The power coefficient can be expressed in terms of the β and λ [9]:

$$C_p(\lambda,\beta) = c_1\left(\frac{c_2}{\lambda_i} - c_3\beta - c_4\right)e^{\frac{-c_5}{\lambda_i}} + c_6\lambda \quad (3)$$

With: $c_1 = 0.5176,\ c_2 = 116,\ c_3 = 0.4,\ c_4 = 5,$

$c_5 = 21,\ c_6 = 0.0068.$

Where λ_i is given by

$$\frac{1}{\lambda_i} = \left(\frac{1}{\lambda+0.08\beta} - \frac{0.035}{\beta^3+1}\right) \quad (4)$$

And the tip speed ratio λ is [10]:

$$\lambda = \frac{\omega_t.R}{v} = \frac{\omega_r.G.R}{v} \quad (5)$$

B. DFIG Model

In rotating field reference frame, the Park's transformation and two-phase reference model of the wound rotor induction machine are shown respectively in Figures 2 and 3:

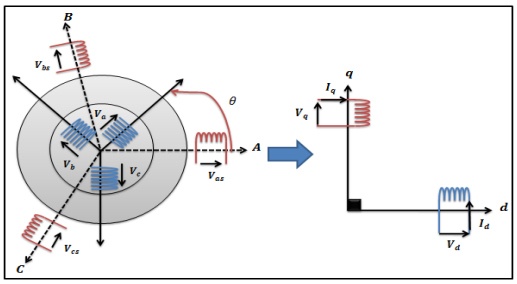

Fig. 2: Park's Model of the DFIG

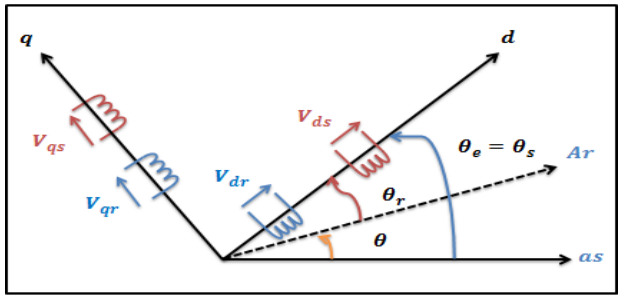

Fig. 3: Representation of the DFIG in the two-phase reference

Electromagnetic and mechanical torques equations are [11]:

$$\begin{cases} T_e = -\frac{3}{2}P\frac{L_m}{L_s}\left(\varphi_{ds}I_{dr} - \varphi_{qs}I_{ds}\right) \\ J\frac{d\Omega_r}{dt} + f\Omega_r = T_e - T_m \end{cases} \quad (6)$$

Equations of stator, rotor voltage and flux components are [11]:

$$\begin{cases} V_{ds} = R_sI_{ds} + \frac{d\varphi_{ds}}{dt} - \omega_s\varphi_{qs} \\ V_{qs} = R_sI_{qs} + \frac{d\varphi_{qs}}{dt} - \omega_s\varphi_{ds} \\ V_{dr} = R_rI_{dr} + \frac{d\varphi_{dr}}{dt} - (\omega_s - \omega_r)\varphi_{qr} \\ V_{qr} = R_rI_{qr} + \frac{d\varphi_{qr}}{dt} - (\omega_s - \omega_r)\varphi_{dr} \end{cases} \quad (7)$$

$$\begin{cases} \varphi_{ds} = L_sI_{ds} + L_mI_{dr} \\ \varphi_{qs} = L_sI_{qs} + L_mI_{qr} \\ \varphi_{dr} = L_rI_{dr} + L_mI_{ds} \\ \varphi_{qr} = L_rI_{qr} + L_mI_{qs} \end{cases} \quad (8)$$

III. DFIG Control Of Active And Reactive Power

Figure 4 shows the direct control loop of the active and reactive power of the DFIG. To achieve a stator active and reactive power vector control, $d-q$ reference frame synchronized with the stator flux has been chosen [12]-[14]. By setting the stator flux vector aligned with d axis, $\varphi_{ds} = \varphi_s$ and $\varphi_{qs} = 0$ [12]-[14].

$$T_e = -\frac{3}{2}P\frac{L_m}{L_s}(\varphi_{ds}I_{dr}) \quad (9)$$

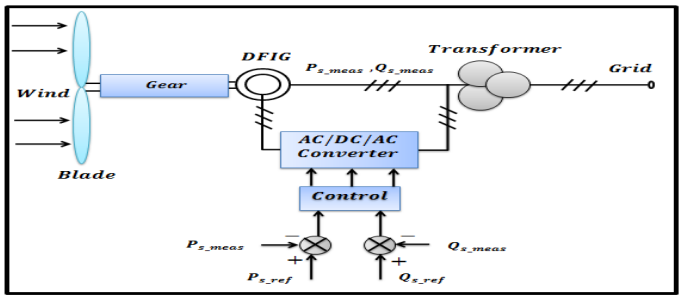

Fig. 4: Power Direct Control between the stator and the grid

Torque in (9) represents a disturbance for the wind turbine and takes a negative value. The electromagnetic torque and the active power depend only on the q-axis rotor current. Neglecting the per phase stator resistance R_s (that's the case for medium and high power machines used in wind energy conversion systems) [12]-[13]-[14], the stator fluxes and voltages can be rewritten as follows [12]-[14]:

$$\begin{cases} \varphi_{ds} = \varphi_s = L_sI_{ds} + L_mI_{dr} \\ \varphi_{qs} = 0 = L_sI_{qs} + L_mI_{qr} \end{cases} \quad (10)$$

$$\begin{cases} V_{ds} = 0 \\ V_{qs} = V_s = \omega_s\varphi_{ds} \end{cases} \quad (11)$$

The stator active and reactive power and rotor voltage are given by:

$$\begin{cases} P_s = V_{ds}I_{ds} + V_{qs}I_{qs} = -V_s\frac{L_m}{L_s}I_{qr} \\ Q_s = V_{qs}I_{ds} - V_{ds}I_{qs} = -V_s\frac{L_m}{L_s}I_{dr} + V_s\frac{\varphi_s}{L_s} \end{cases} \quad (12)$$

$$\begin{cases} V_{dr} = R_r I_{dr} + L_r \sigma \frac{d}{dt} I_{dr} - g\omega_s L_r \sigma I_{qr} \\ V_{qr} = R_r I_{qr} + L_r \sigma \frac{d}{dt} I_{qr} + g\omega_s L_r \sigma I_{dr} + g \frac{L_m V_s}{L_s} \end{cases} \quad (13)$$

$$\sigma = \left(1 - \frac{L_m^2}{L_s L_r}\right) \quad (14)$$

In steady state, the second derivative terms in equation 13 are nil. The third term constitutes cross coupling terms. The block diagram representing the internal model of the system is shown in Figure 5.

The input blocks relating V_{dr} to V_{qr} represent the simplified rotor converter model. Knowing equations 12 and 13, it is then possible to synthesize the regulators.

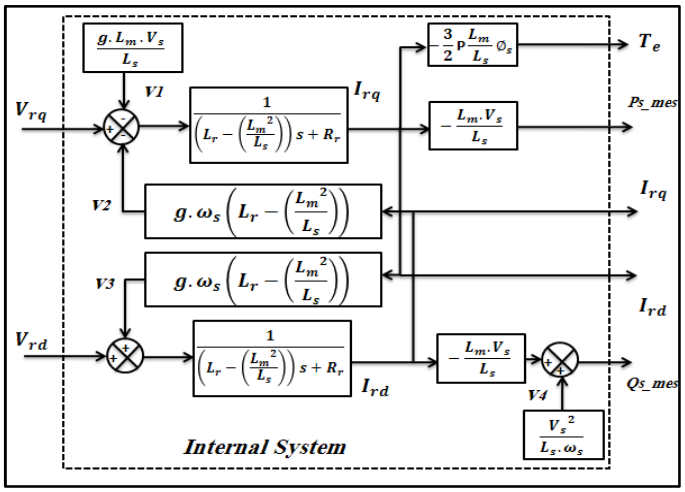

Fig. 5: Block diagram representation

IV. CONTROLLERS DESIGN

All controllers (PI, Fuzzy-PI and SM) are designed to achieve the following control objectives [14]:

- Performing active and reactive power reference tracking;
- Efficient disturbance rejection ;
- Parametric robustness.

A. PI controller design

The block diagram of the power control loop is shown in Figures 6 and 7 [12]**:**

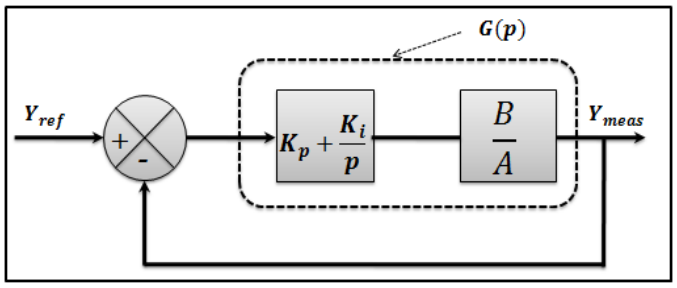

Fig. 6: The structure of PI controller

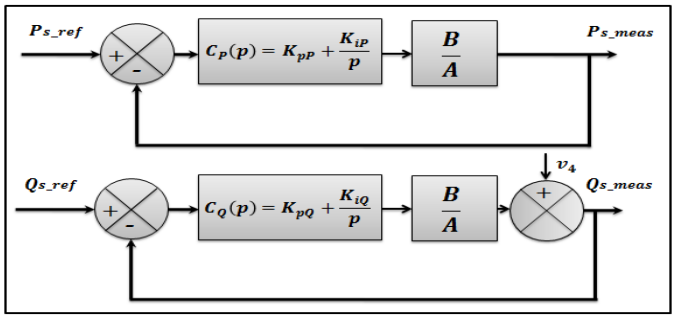

Fig. 7: Equivalent PI control scheme

To keep the property of symmetry of the open-loop, the controllers' gains are voluntary chosen symmetric [10]-[12]:

$$\begin{cases} K_{pp} = K_{pq} = K_p \\ K_{ip} = K_{iq} = K_i \end{cases} \quad (15)$$

And the terms of A and B are [10]-[12]:

$$\begin{cases} A = R_r + sL_r\left(1 - \frac{L_m^2}{L_s L_r}\right) \\ B = \frac{L_m V_s}{L_s} \end{cases} \quad (16)$$

The open loop transfer function of with regulators is [10]:

$$G(p) = \left(\frac{s + \frac{K_i}{K_p}}{\frac{s}{K_p}}\right).\left(\frac{\frac{L_m V_s}{L_r L_s \sigma}}{s + \frac{L_s R_r}{L_r L_s \sigma}}\right) \quad (17)$$

To eliminate the zero of the transfer function, the compensation method was chosen. Then [10]:

$$\frac{K_i}{K_p} = \frac{R_r}{L_r \sigma} \quad (18)$$

The open loop transfer function becomes [10]:

$$G(p) = \frac{K_p \frac{L_m V_s}{L_r L_s \sigma}}{s} \quad (19)$$

The closed loop transfer function is expressed by [10]:

$$H(p) = \frac{1}{1 + s\tau_r} \quad (20)$$

$$\tau_r = \frac{1}{K_p} \frac{L_r L_s \sigma}{L_m V_s} \quad (21)$$

$$\begin{cases} K_p = \frac{L_r L_s \sigma}{\tau_r L_m V_s} \\ K_i = \frac{L_s R_r}{\tau_r L_m V_s} \end{cases} \quad (22)$$

B. Fuzzy-PI controller design

According to the operational features and control requirements of DFIG, a Fuzzy-PI control strategy was developed as shown in Figure 8 [7]-[9]-[18]. The Gain Scheduling method is used.

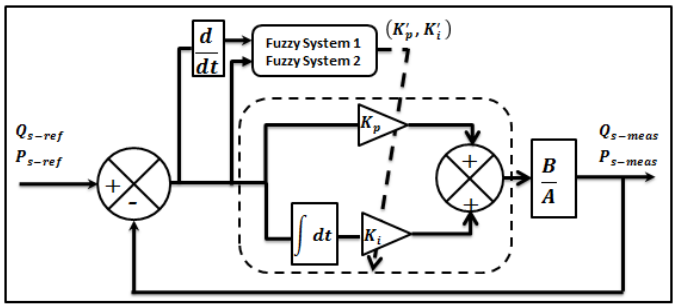

Fig. 8: Structure of Fuzzy-PI control

The Fuzzy controller adjusts the parameters (K_p, K_i) of the PI and generates new parameters so that it fits all operating conditions, based on the error and its derivative [16]-[18].

The PI controller parameters are normalized in the interval $K_p \in [0-5]$; $K_i \in [0-0{,}6]$ using the following linear transformations [11]:

$$\begin{cases} K_p^{'} = (K_p - K_{pmin})/(K_{pmax} - K_{pmin}) \\ K_i^{'} = (K_i - K_{imin})/(K_{imax} - K_{imin}) \end{cases} \quad (23)$$

The inputs of fuzzy controller are: error (e) and its derivative (de/dt), the outputs are: the normalized value of the proportional action ($K_p^{'}$) and the normalized value of the integral action ($K_i^{'}$).

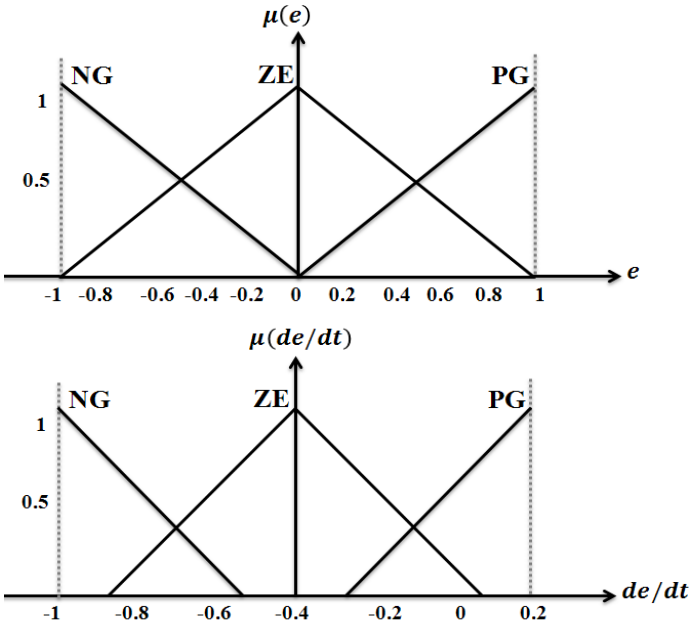

Fig. 9: Membership functions of error and its variation

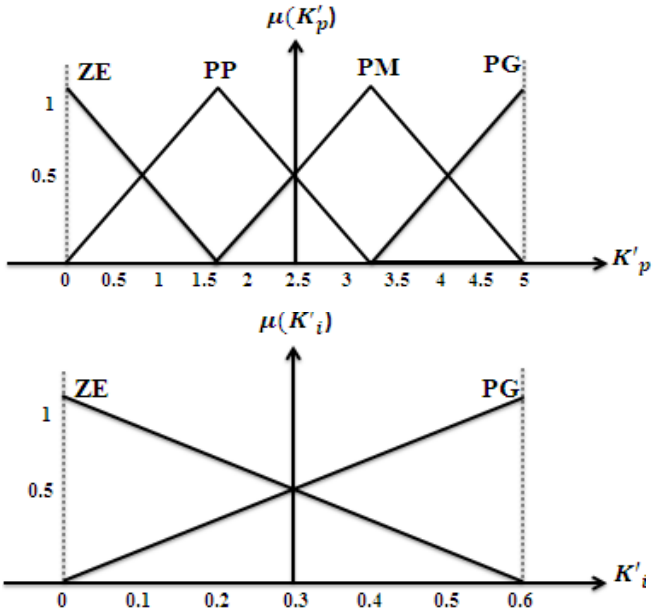

Fig. 10: Membership functions for $K_p'$and K_i'

The input signals have 3 membership functions, while the proportional gain $K_p^{'}$ has 4 and the integral gain $K_i^{'}$ has 2. The three membership functions of the active and reactive power controllers of input signals are represented in Figure 9.

The membership functions for the proportional gain $K_p^{'}$ and the integral gain $K_i^{'}$ of the active and reactive power controller are represented in Figure 10. The fuzzy rules of the active and reactive power controllers are shown Tables1 and 2.

TABLE 1: THE RULE BASE OF FUZZY CONTROLLER FOR K_p'

U		e		
		NB	ZE	PB
de	NB	ZE	ZE	ZE
	ZE	PB	PS	PB
	PB	ZE	PM	ZE

TABLE 2: THE RULE BASE OF FUZZY CONTROLLER FOR K_i'

U		e		
		NB	ZE	PB
de	NB	PB	PB	PB
	ZE	ZE	PB	Z
	PB	PB	PB	PB

Negative Big = NB; Zero = ZE; Positive Big = PB; Positive Medium = MP; Positive Small = PS.

C. Sliding Mode controller design

The Sliding Mode (SM) controller has been very successful in recent years due to the simplicity of its implementation and its robustness against the uncertainties of the system and external disturbances in the process.

Sliding mode control brings back the state trajectory to the sliding surface [1]-[15]-[17]. It can be applied to

active and reactive powers which can be expressed as the derivative of sliding surface

$$\begin{cases} \dot{S}(P) = \left(\dot{P}_{s-ref} - \dot{P}_{s-mes}\right) \\ \dot{S}(Q) = \left(\dot{Q}_{s-ref} - \dot{Q}_{s-mes}\right) \end{cases} \quad (24)$$

From equation 12, the derivative expressions of active and reactive power are:

$$\begin{cases} \dot{S}(P) = \left(\dot{P}_{s-ref} - V_s \frac{L_m}{L_s} \dot{I}_{rq}\right) \\ \dot{S}(Q) = \left(\dot{Q}_{s-ref} - V_s \frac{L_m}{L_s} \dot{I}_{rd}\right) \end{cases} \quad (25)$$

$$\begin{cases} \dot{S}(P) = \left(\dot{P}_{s-ref} - V_s \frac{L_m}{L_s L_r \sigma} \left(V_{rq} - R_r I_{rq}\right)\right) \\ \dot{S}(Q) = \left(\dot{Q}_{s-ref} - V_s \frac{L_m}{L_s L_r \sigma} \left(V_{rd} - R_r I_{rd}\right)\right) \end{cases} \quad (26)$$

During the sliding mode and steady state, we have:

$$\begin{cases} S(P) = 0 \; and \; S(Q) = 0 \\ \dot{S}(P) = 0 \; and \; \dot{S}(Q) = 0 \\ V_{rq}^n = 0 \quad and \quad V_{rd}^n = 0 \end{cases} \quad (27)$$

Replacing V_{qr} by $V_{qr}^{eq} + V_{qr}^n$, and V_{dr} by $V_{dr}^{eq} + V_{dr}^n$, equation (26) becomes:

$$\begin{cases} \dot{S}(P) = \left(\dot{P}_{s-ref} - V_s \frac{L_m}{L_s L_r \sigma} \left(V_{rq}^{eq} + V_{rq}^n - R_r I_{rq}\right)\right) \\ \dot{S}(Q) = \left(\dot{Q}_{s-ref} - V_s \frac{L_m}{L_s L_r \sigma} \left(V_{rd}^{eq} + V_{rd}^n - R_r I_{rd}\right)\right) \end{cases} \quad (28)$$

Then the equivalent command V_{qr}^{eq} and V_{dr}^{eq} can be written as:

$$\begin{cases} V_{rq}^{eq} = \left(-\dot{P}_{s-ref} \frac{L_s L_r \sigma}{L_m V_s} + R_r I_{rq}\right) \\ V_{rd}^{eq} = \left(-\dot{Q}_{s-ref} \frac{L_s L_r \sigma}{L_m V_s} + R_r I_{rd}\right) \end{cases} \quad (29)$$

During the convergence mode, the condition for power; $S(P)\dot{S}(P) \leq 0$ and $S(Q)\dot{S}(Q) \leq 0$ is verified, we set:

$$\begin{cases} \dot{S}(P) = \left(-V_s \frac{L_m}{L_s L_r \sigma} V_{rq}^n\right) \\ \dot{S}(Q) = \left(-V_s \frac{L_m}{L_s L_r \sigma} V_{rd}^n\right) \end{cases} \quad (30)$$

Therefore, the switching term is given by:

$$\begin{cases} V_{rq}^n = K_1 sign\left(S(P)\right) \\ V_{rd}^n = K_2 sign\left(S(Q)\right) \end{cases} \quad (31)$$

To verify the condition of stability of the system, parameters K_1 and K_2 must be positive. To mitigate the overshoot of the reference voltage V_{qr} and V_{dr}, it is often useful to add a voltage limiter.

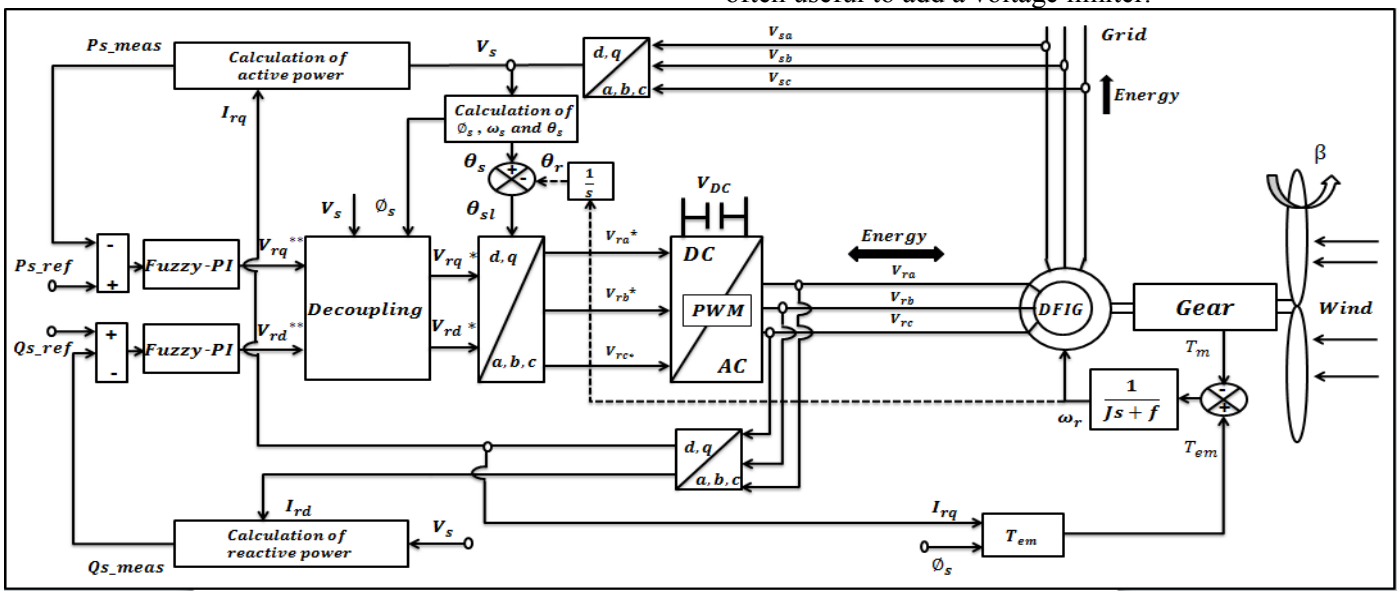

Fig. 11: Direct control loop of DFIG using Fuzzy-PI

V. Simulation Results

To analyze the system and compare efficiently the two proposed controllers, a set of simulations have been performed using Matlab/Simulink/SimPowerSystems environment. The PWM inverter on the rotor side of the DFIG ($P_m = 1.5\ MW$) is controlled. Both controllers are tested and compared by two different criteria, namely, reference tracking and robustness by varying the parameters of the system. WECS system's parameters are listed respectively in Tables 3, 4, and 5.

A. Power Electronic Converters of the DFIG

Figure 12 presents the simulation results of the rectifier and the filter.
$V_a(t), V_b(t)$ and $V_c(t)$ are respectively the input voltages of the grid.
$V_{red}(t)$ is output voltage of the rectifier.
$V_{dc}(t)$ is output voltage of the A low-pass (LC) filter.

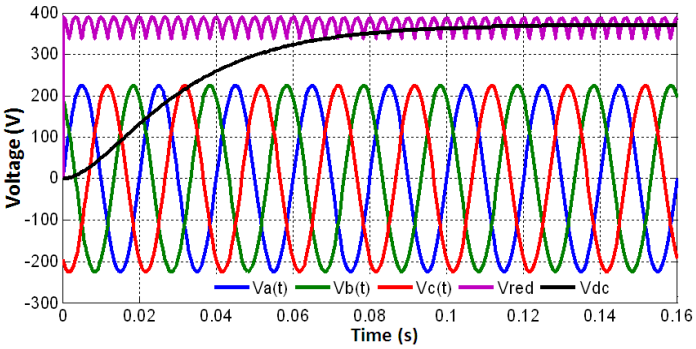

Fig. 12: Input and output voltages of the rectifier and filter

The output voltage of the inverter controlled by Pulse Width Modulation (PWM) is presented in Figure 13 [19].

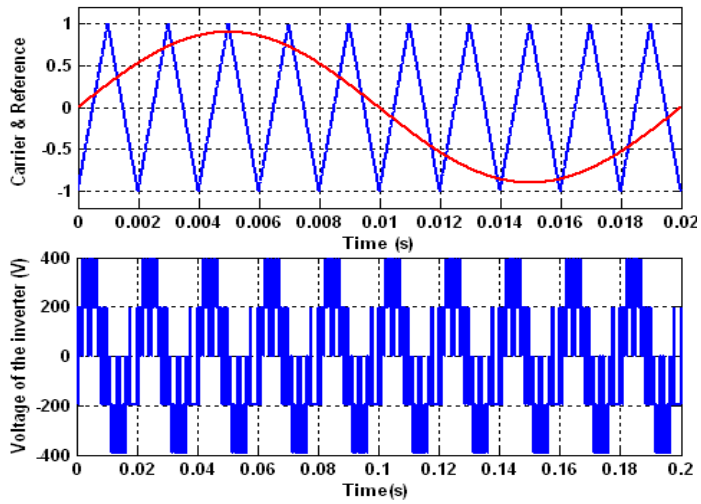

Fig.13: Simulation results of the Power Rotor

B. Reference tracking

The machine is first tested as in ideal conditions mode and driven to $\omega_s = 1500\, rmp$. Different step inputs for an active and a reactive power were applied and the dynamic responses for PI, Fuzzy-PI and the SM controllers are illustrated in Figure 14.

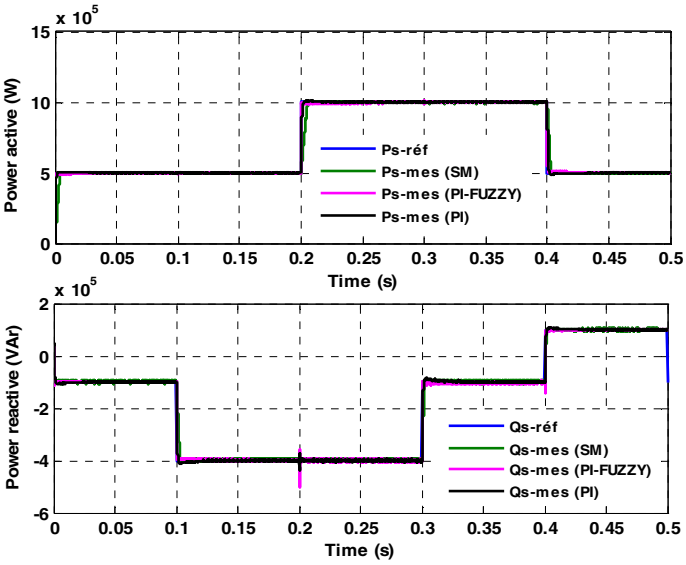

Fig.14: Dynamic Responses of PI, Fuzzy-PI and SM controllers to the active and reactive power step change using

Through the comparative study, we can conclude that the various regulators SM, PI and Fuzzy-PI give almost the same results for the different tests applied to the DFIG, but with better transient response time in the case of the Fuzzy-PI. The steps are correctly followed and there is no more error on the powers. The decoupling between the two powers is perfectly respected. The negative sign of the reactive power shows that the machine operates in generator mode; for drive mode, the reactive power becomes automatically positive.

C. Robustness

In order to investigate the robustness of the controllers, the value of the R_r is doubled from its nominal value. The value of L_s and L_r are increased by 10% of their nominal values and the value of L_m is decreased by 10% of its nominal value.

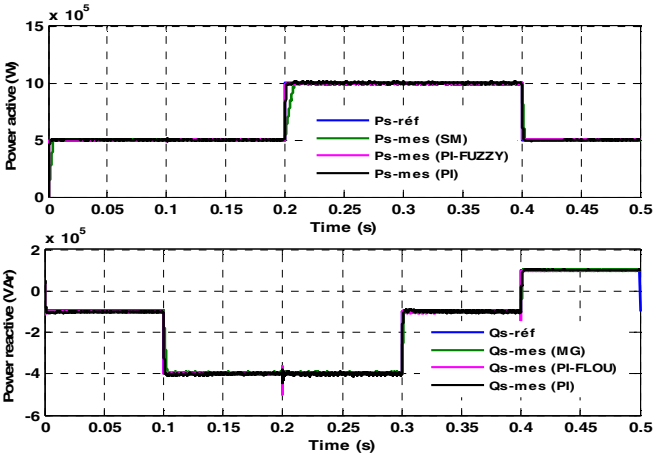

Fig.15: Active and reactive power behavior using PI, Fuzzy-PI and SM controllers with R_r 50% Variation

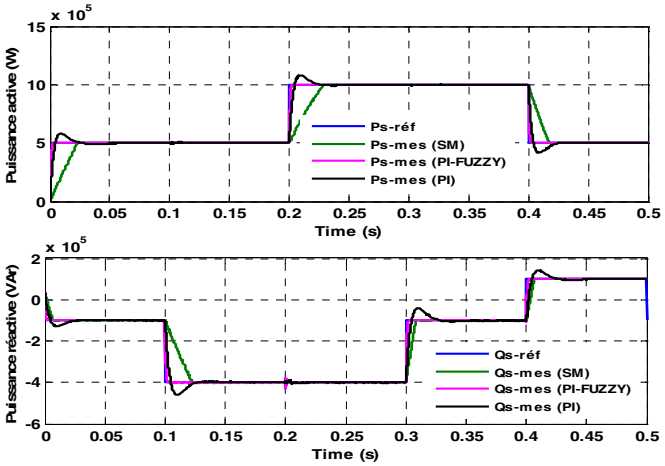

Fig.16: Active and reactive power behavior using PI, Fuzzy-PI and SM controllers with L_s +10% Variation

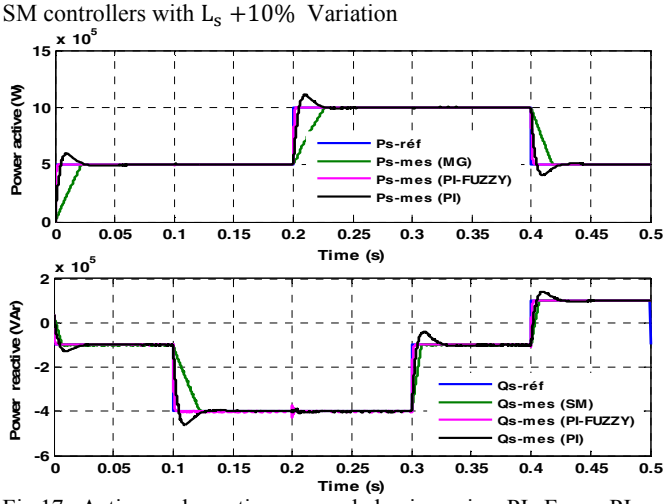

Fig.17: Active and reactive power behavior using PI, Fuzzy-PI and SM controllers with L_r +10% Variation

The effect of parameters variation on the active and reactive power was investigated for the controllers (Figures 15, 16, 17). The objective of robustness tests is to compare the performance of the controllers when machine's parameters change.

Figure 18 shows simulation results when several parameters (R_r+50 %, L_s+20 %, L_r +20 % and L_m -20 %) change at the same time. The obtained simulation results indicate the best performances for the adaptive fuzzy-PI controller.

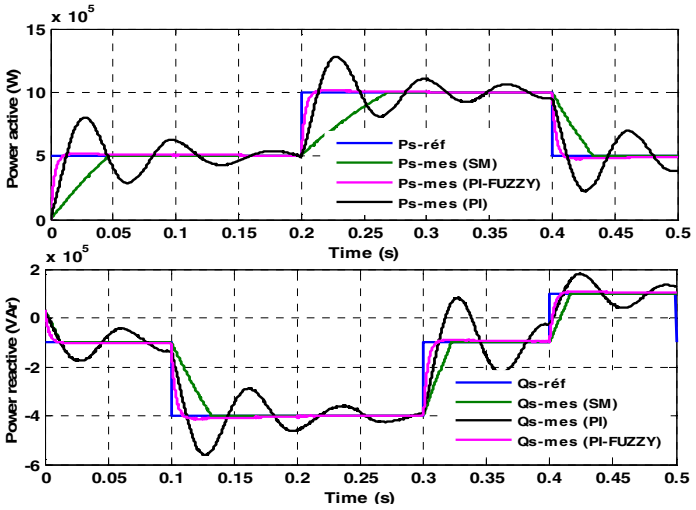

Fig.18: Active and reactive power behavior using PI, Fuzzy-PI and SM controllers with simultaneously variation of parameters

For the Fuzzy-PI, the response time is significantly reduced and the oscillations are limited and damped more quickly compared to other controllers.

D. Comparison of the behavior of the three controllers

For stepped changes of active and reactive powers, the Fuzzy-PI controller gave the best transient result (Figure 19).

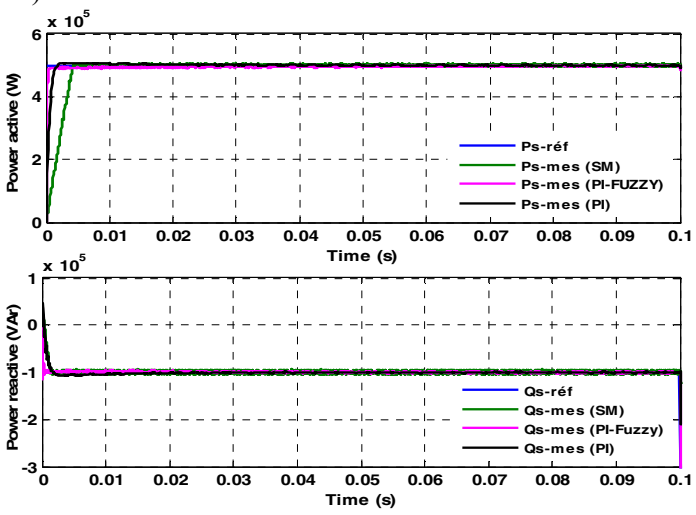

Fig.19: Comparative response of the active and reactive power using the PI, Fuzzy-PI and SM controllers

VI. CONCLUSION

In this paper, a decoupled control method of active and reactive powers for a DFIG was developed. The global model of the system and vector control strategy, were first established. Furthermore, three types of controllers (Proportional-Integral, Fuzzy-Proportional-Integral and Sliding Mode) were designed to perform power reference tracking and robustness to machine parameters variation. The results show that, with Fuzzy-

PI, the settling time is reduced considerably, peak overshoot of values are limited and oscillations are damped out faster. The transient response provided by the Fuzzy-PI has been best compared to conventional PI and SM controllers.

TABLE 3: WECS PARAMETERS

Symbol	Value
Stator rated voltage Vs	$398 / 690\ Volt$
Rated frequency stator fs	$50\ Hz$
Rotor rated voltage Vr	$225 / 389\ Volt$
Rated frequency stator fr	$14\ Hz$
Stator resistance R_s	$0.012\ \Omega$
Rotor resistance R_r	$0.021\ \Omega$
Pole Pairs P	2
Stator inductance L_s	$0.0137\ H$
Rotor inductance L_r	$0.0136\ H$
Mutual inductance L_m	$0.0135\ H$
The friction coefficient f	$0.0024\ N.m.s^{-1}$
The moment of inertia J	$1000\ kg.m^2$
Radius of the wind R	$35.25\ \ m$
Gain multiplier G	90
Air density ρ	$1.225\ \ kg/m^3$

TABLE 4: PI CONTROLLER PARAMETERS

Symbol	Value
Gain K_i	$7.575e-4$
Gain K_p	$535.455e-4$

TABLE 5: SMC PARAMETERS

Symbol	Value
Gain K_1	500
Gain K_2	150
Value of Saturation	± 110
Fixed-step size	$2e-5$

REFERENCES

[1] J. Soltani, A. Farrokh Payam, "A Robust Adaptive Sliding-Mode Controller for Slip Power Recovery Induction Machine Drives," *IEEE Trans. Power Electronics and Motion Control Conference, vol.3,* pp. 3-8, 2006.

[2] Sergei Peresada, Andrea Tilli and, Alberto Tonielli, "Indirect Stator Flux-Oriented Output Feedback Control of a Doubly Fed Induction Machine*," IEEE Trans. Control Systems Technology, vol.11,* pp.875-888, Nov 2003.

[3] Gilbert C, D. Sousa and, B. K. Bose, "Fuzzy logic applications to power electronics and drives - an overview," *Proceedings of IECON 1995*, Nov 1995, pp.57-62.

[4] J. G. Slootweg, H. Polin der and, W. L. Kling, "Initialization of wind turbine models in power systems dynamic simulations," *IEEE Power Tech Conference, Porto Portugal, Vol. 3,* 6 pp, Sep 2001.

[5] Zhou D, Mu C D and, Xu W L, "Adaptive sliding mode guidance of a homing missile", *Jounal of guidance, control and dynamics, vol. 22, no. 4*, , 1999,pp. 589-592.

[6] A. G. Ram, S. and A. Lincoln, "Fuzzy adaptive PI controller for single input single output non-linear system," *ARPN Journal of Engineering and Applied, Sciences. Vol. 7, NO. 10,* pp. 1273 – 1280, 2012.

[7] H. M. Soloumah and N. C. Kar, "Fuzzy logic based vector control of a doubly-fed induction generator for wind power application," *IEEE Trans .Wind Engineering, vol. 30, no. 3,* pp. 201-224, 2006.

[8] Siegfried Heier, *Grid Integration of Wind Energy Conversion Systems,* John Wiley & Sons Ltd, ISBN 0-471-97143-X, 1998.

[9] Yao Xing-jia, Liu Zhong-liang, Cui Guo-sheng "Decoupling Control of Doubly-Fed Induction Generator based on Fuzzy-PI Controller,*" IEEE Trans. Mechanical and Electrical Technology* (ICMET 2010) , pp 226-230 ,2010.

[10] T.D. Mai, B.L. Mai, D.T. Pham, and H.P. Nguyen: "Control of doubly-fed induction generators using Dspace R&D controller board – an application of rapid control coordinated with Matlab/Simulink ," October 2007, *International Symposium on Electrical & Electronics Engineering*, Track. 3, pp 302-307.

[11] L. Zhang, C. Watthansarn and W. Shehered: "A matrix converter excited doubly-fed induction machine as a wind power generator," *IEEE Trans.Power Electronics and Variable Speed Drives, vol. 2, pp 532 - 537,* 06 August 2002.

[12] F. Poitiers, M. Machmoum, R. Le Daeufi and M.E. aim, "Control of a doubly-fed induction generator for wind energy conversion systems," *IEEE Trans .Renewable Energy, Vol. 3, N°. 3, pp.373-378, December 2001*.

[13] T.J.Porcyk and E.H.Mamdani, "A linguistic self-organizing process controller," *Automatica, vol.15, pp.15-30, 1979*.

[14] M. Machmoum, F. Poitiers, C. Darengosse and A. Queric, "Dynamic Performances of a Doubly-fed Induction Machine for a Variable-speed Wind Energy Generation," *IEEE Trans. Power System Technology, vol. 4, pp. 2431-2436, Dec. 2002*.

[15] Md. Rabiul Islam1, Youguang Guo, Jian Guo Zhu, "Steady State Characteristic Simulation of DFIG for Wind Power System," *IEEE Trans. Electrical and Computer Engineering (ICECE), pp. 151-154, 2011*.

[16] Hong Hee Lee, Phan Quoc Dzung, Le Minh Phuong, Le Dinh Khoa, Nguyen Huu Nhan ,"A New Fuzzy Logic Approach For Control System Of Wind Turbine With Doubly Fed Induction Generator," *IEEE Trans Strategic Technology (IFOST),6 pp, 2010.*

[17] J.J.Slotine, "Adaptive Sliding controller synthesis for nonlinear systems *", IJC, Vol 43 .N°6, 1986, pp 1631-1651*.

[18] A. G. Ram, S. and A. Lincoln, "Fuzzy adaptive PI controller for single input single output non-linear system," *ARPN Journal of Engineering and Applied, Sciences. VOL. 7, NO. 10*, pp. 1273 – 1280, 2012.

[19] M. Messaouda, and A. Ouddane, *Contrôle des Puissances Actives et Réactives de la MADA intégrée dans un Système Eolien* , Master thesis in automatic department of automatic University Mohamed Boudiaf USTO, June 2011.